2012 IEEE International Conference on Robotics and Automation
RiverCentre, Saint Paul, Minnesota, USA
May 14-18, 2012

# Rolling Tensegrity Driven by Pneumatic Soft Actuators

Yuusuke Koizumi, Mizuho Shibata, and Shinichi Hirai

*Abstract*— **In this paper, we describe the rolling of a tensegrity robot driven by a set of pneumatic soft actuators. Tensegrity is a mechanical structure consisting of a set of rigid elements connected by elastic tensional elements. Introducing tensegrity structures, we are able to build soft robots with larger size. Firstly, we show the prototype of a six-strut tensegrity robot, which is driven by twenty-four pneumatic McKibben actuators. Second, we formulate the geometry of the tensegrity robot. We categorize contact states between a six-strut tensegrity robot and a flat ground into two; axial symmetric contact and planar symmetric contact. Finally, we experimentally examine if rolling can be performed over a flat ground for individual sets of the actuators and discuss the strategy of rolling.**

## I. Introduction

This paper focuses on the rolling of a tensegrity robot driven by a set of pneumatic soft actuators.

Recently, locomotion of soft material robots has been studied extensively [1], [2], [3], [4], [5], [6]. Robots made of soft material may be able to change their shape for rough terrain locomotion, obstacle avoidance, and narrow passage locomotion. Robots may be able to utilize elastic energy stored in soft material for their locomotion and jumping. On the other hand, it is difficult to build larger robot bodies due to natural deformation of soft material. We need to introduce *bones* into soft robots to build larger ones. Conventionally, robotics has been applying link mechanisms, where rigid bodies are linked one another through mechanical joints, to robot bodies. Link mechanisms can be embedded into soft material robots, but such link mechanisms may hinder the deformation of the soft robots; link mechanisms tend to be heavy weighted, not only due to link weight but also due to complicated joint mechanisms. To cope with this dilemma, we proposed to apply *tensegrity* structures to soft robots [7], [8].

*Tensegrity* is a mechanical structure consisting of a set of rigid elements connected by elastic tensional elements. Rigid elements, which are referred to as *struts*, are disconnected one another. The structure keeps its shape due to the balance among the tensile and compressive forces applied to the structure. Tensegrity is an abbreviation of *tensile integrity*. Tensegrity structure is firstly proposed in architecture [9], [10]. Tensegrity structures are lightweight and flexible; they are applied to architectural designs of bridges and domes. In architecture, many studies have been conducted to investigate the properties of tensegrities [11], [12], [13]. The concept of tensegrity has been applied not only to architecture but also other areas including biology and robotics. In biology, tensegrity structures were applied to the description of living cells [14]. In robotics, tensegrities are applied to lightweight robotic arms [15] and locomotion robots [16], [17]. In addition, Kinematics and statics of a modular tensegrity mechanism was analyzed [18].

Y. Koizumi and S. Hirai are with the Department of Robotics, Ritsumeikan University, Kusatsu, Shiga 525–8577, Japan. hirai@se.ritsumei.ac.jp

M. Shibata is with the Department of Intelligent Mechanical Engineering, Kinki University, Higashi Hiroshima, Hiroshima 739–2116, Japan.

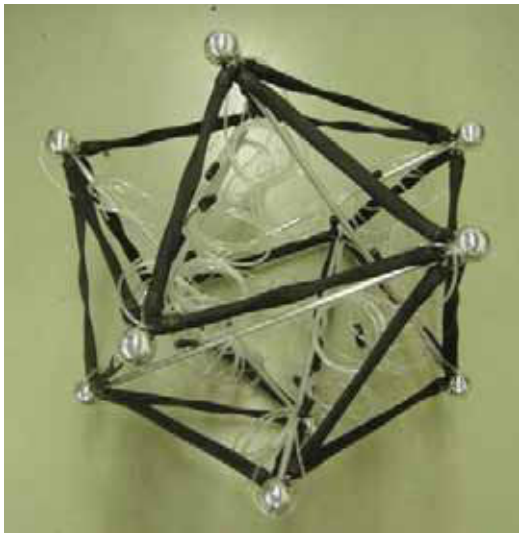

Fig. 1. Prototype of six-strut tensegrity robot. The prototype consists of 6 rigid struts and 24 pneumatic McKibben actuators. Two rigid balls are attached to the both ends of each strut. Air pressure to the actuators is applied externally through hoses.

In [7], [8], we have built a tensegrity robot prototype of almost 150 mm in size. The size is limited due to SMA actuators applied to the prototype. In this paper, we build a tensegrity robot prototype of almost 600 mm in size. We will apply pneumatic soft actuators, which can generate larger forces than SMA actuators can, into the tensegrity robot prototype. Also, we will examine if the prototype can perform successive rolling over the ground. The rest of this manuscript is organized as follows. Section II introduces rolling tensegrity robots and their geometric description. Section III briefly describes the dynamics of tensegrity robot rolling. Section IV shows experimental results. Finally, section V provides conclusion and future works.

## II. Rolling Tensegrity Robot

### A. Six-strut Tensegrity Robot

Figure 1 shows a prototype of a six-strut tensegrity robot. This prototype consists of 6 rigid struts and 24 pneumatic McKibben actuators. Note that McKibben actuators exhibit

978-1-4673-1405-3/12/$31.00 ©2012 IEEE

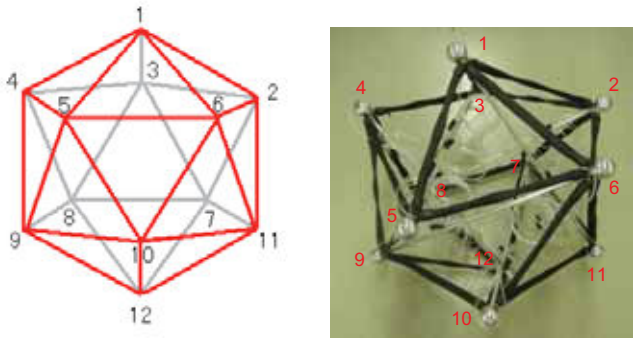


(a) (b)

Fig. 2. Geometry of six-strut tensegrity robot. (a) A six-strut tensegrity forms an icosahedron, consisting of eight regular triangles and twelve non-regular, isosceles triangles. (b) Numbers are attached to individual vertices of a tensegrity robot prototype.

elasticity in their expansion, working as tensional elements of a tensegrity structure.

Assume that a tensegrity robot lies on a flat ground. A tensegrity structure deforms under gravity to achieve a stable state, where the gravitational potential energy reaches to its local minimum. Applying air pressure, each McKibben actuator shrinks, making the imbalance among forces in the tensegrity robot. Then, the robot starts to roll, guided into another stable state. Releasing the applied air pressure, the tensegrity structure returns to its natural shape. A successive application of air pressure to appropriate McKibben actuators yields a successive rolling of the tensegrity robot on the ground.

A six-strut tensegrity forms an icosahedron, consisting of eight regular triangles and twelve non-regular, isosceles triangles. Each stable state is realized when its corresponding triangle is in contact with the ground. In other words, each stable state is specified by its corresponding triangle in contact with the ground. During the rolling locomotion of this six-strut tensegrity robot on a flat ground, each of the twenty triangles contacts to the ground, implying that the locomotion can be described by a sequence of transitions among stable states, each of which corresponds to a triangle.

### B. Geometric Description of Tensegrity

Let us attach numbers to individual vertices of a six-strut tensegrity robot, as illustrated in Figure 2-(a). This numbering is based on the standard in geometry [19]. Vertex numbers of our prototype is shown in Figure 2-(b). Then, each strut is specified by a pair of vertices at its both ends. For example, strut between vertices 1 and 11 is described as $(1,11)$. Vertices for individual struts are listed in Table I. Also, each McKibben actuator is specified by a pair of vertices at its both ends. For example, actuator connecting vertices 1 and 6 is specified by $(1,6)$. Vertices for individual actuators are listed in Table II.

Let us look at a triangle of a six-strut tensegrity robot from outside and follow its vertices counterclockwise. Each regular triangle is specified by a triplet of vertices. For example, a regular triangle consisting of vertices 1, 5, and 6 is specified by $(1,5,6)$. A regular triangle $(1,5,6)$ has three actuators along its all edges. Each non-regular, isosceles triangle is specified by a triplet of vertices as well. The first vertex of the triplet denotes the vertex opposite to the base. The base is specified by a pair of the second and third vertices. For example, a non-regular, isosceles triangle $(1,6,2)$ consists of vertex 1 and base $(6,2)$. A non-regular, isosceles triangle $(1,6,2)$ has two actuators along $(1,6)$ and $(2,1)$ but no actuator along base $(6,2)$. Vertices for individual regular triangles are listed in Table III-(a) and vertices for individual non-regular, isosceles triangles are listed in Table III-(b).

TABLE I

STRUTS AND CORRESPONDING VERTICES

| strut # | vertices | |
|---|---|---|
| 1 | 1 | 11 |
| 2 | 2 | 8 |
| 3 | 3 | 5 |
| 4 | 4 | 12 |
| 5 | 6 | 9 |
| 6 | 7 | 10 |

TABLE II

ACTUATORS AND CORRESPONDING VERTICES

| actuator # | vertices | |
|---|---|---|
| 1 | 1 | 2 |
| 2 | 1 | 3 |
| 3 | 1 | 5 |
| 4 | 1 | 6 |
| 5 | 2 | 3 |
| 6 | 2 | 7 |
| 7 | 2 | 11 |
| 8 | 3 | 4 |
| 9 | 3 | 8 |
| 10 | 4 | 5 |
| 11 | 4 | 8 |
| 12 | 4 | 9 |

| actuator # | vertices | |
|---|---|---|
| 13 | 5 | 6 |
| 14 | 5 | 9 |
| 15 | 6 | 10 |
| 16 | 6 | 11 |
| 17 | 7 | 8 |
| 18 | 7 | 11 |
| 19 | 7 | 12 |
| 20 | 8 | 12 |
| 21 | 9 | 10 |
| 22 | 9 | 12 |
| 23 | 10 | 11 |
| 24 | 10 | 12 |

### C. Description of Contacts

Recalling that a six-strut tensegrity forms an icosahedron, consisting of eight regular triangles and twelve non-regular, isosceles triangles, we find that the tensegrity robot contacts with the flat ground through one of the twenty triangles. In other words, we have 20 stable states in the rolling of a six-strut tensegrity robot on the flat ground and each state can be specified by a triangle contacting to the ground. Note that each regular triangle has three actuators while each non-regular, isosceles triangle has two actuators.

Figure 3 shows one stable state where a regular triangle is in contact with the flat ground. The figure exhibits the front, side, and top views of the natural shape of a tensegrity robot in the stable state. As shown in the figure, the natural shape of the tensegrity robot is axial symmetric with respect to a normal to the flat ground. The natural shape is symmetric around the normal by angle of $2\pi/3$. Such stable state is referred to as *axial symmetric contact* in this paper. On the other hand, Figure 4 shows one stable state where a non-regular, isosceles triangle is in contact with the flat ground. As shown in the figure, the natural shape of the

TABLE III

TRIANGLES AND CORRESPONDING VERTICES

(a) regular triangles

| regular | vertices | | |
|---|---|---|---|
| 1 | 1 | 2 | 3 |
| 2 | 1 | 5 | 6 |
| 3 | 2 | 11 | 7 |
| 4 | 3 | 8 | 4 |
| 5 | 4 | 9 | 5 |
| 6 | 6 | 10 | 11 |
| 7 | 7 | 12 | 8 |
| 8 | 9 | 12 | 10 |

(b) isosceles triangles

| isosceles | vertices | | |
|---|---|---|---|
| 1 | 1 | 6 | 2 |
| 2 | 2 | 7 | 3 |
| 3 | 3 | 4 | 1 |
| 4 | 4 | 8 | 9 |
| 5 | 5 | 1 | 4 |
| 6 | 6 | 5 | 10 |
| 7 | 7 | 11 | 12 |
| 8 | 8 | 3 | 7 |
| 9 | 9 | 10 | 5 |
| 10 | 10 | 12 | 11 |
| 11 | 11 | 2 | 6 |
| 12 | 12 | 9 | 8 |

tensegrity robot is planar symmetric with respect to a plane perpendicular to the flat ground. Such stable state is referred to as *planar symmetric contact* in this paper.

## III. Dynamics of Rolling Tensegrity Robots

The configuration of a six-strut tensegrity robot is given by a set of the position and rotation descriptions of the six struts. Configuration of each strut consists of 6 independent generalized coordinates; 3 for position and 3 for rotation of each strut. Thus, configuration of a six-strut tensegrity robot has 36 independent generalized coordinates. Contact between a tensegrity robot and the flat ground through a triangle imposes geometric constraints into the tensegrity configuration. The internal energy of the tensegrity robot reaches to its local minimum under the constraints at the stable state. In other words, the extended internal energy, which includes the products between Lagrange multipliers and geometric constraints, reaches to its minimum with respect to the tensegrity configuration and the multipliers. Geometric constraints along the normal of the ground are unidirectional, implying that the corresponding multipliers, which represent the normal reaction forces, should be positive or equal to zero.

Applying air pressure to pneumatic actuators affects the internal energy, changing multiplier values. When a multiplier corresponding to any unidirectional constraint exceeds zero, the unidirectional constraint is lost, implying that the contact is lost. This causes the transition from one stable state to one instability, which may lead to another stable state. Transition from one stable state to another thus includes intermediate instability and topological change of geometric constraints imposed on the dynamic equations of motion, which yields the difficulty in analyzing the transitions among stable states. Consequently, we will examine the possibility of transitions through experiment in this paper.

## IV. Experiment on Rolling of Tensegrity Robot

### A. Experimental Setup

We have built up a prototype of a six-strut tensegrity robot shown in Figure 1. Six struts 570 mm in length are made of aluminum. Two rigid balls of diameter 45 mm are attached to the both ends of each strut. We have used McKibben actuators fabricated by Kanda Tsushin Kogyo. The actuators can generate force of 800 N by applying air pressure of 0.5 MPa. Contraction ratio is almost 34 % without any load and 20 % under the load of 3 N by applying air pressure of 0.5 MPa. Air pressure to the actuators is applied externally through air hoses. Height and width of the prototype are 590 mm and 780 mm, respectively, in its natural shape, and its weight is 3.3 kg.

(a) front (b) side (c) top

Fig. 3. Axial symmetry contact. One of eight regular triangles contacts to the ground. The natural shape of the tensegrity structure is axial symmetric with angle of $2\pi/3$.

(a) front (b) side (c) top

Fig. 4. Planar symmetry contact. One of twelve non-regular, isosceles triangles contacts to the ground. The natural shape of the tensegrity structure is planar symmetric.

Recall that applying air pressure to McKibben actuators of a tensegrity robot and releasing the applied air pressure can cause the transitions among stable states. Let us experimentally investigate if transitions are possible or not. We have found that applying air pressure of 0.50 MPa to a single pneumatic McKibben actuator cannot realize the rolling of the tensegrity robot. Based on this preliminary experimental result, we apply air pressure, from 0.05 MPa to 0.50 MPa at the interval of 0.05 MPa, into two pneumatic McKibben actuators at the same time to examine if the prototype rolls. We have recorded the lowest air pressure that can drive the prototype for each pair of McKibben actuators.

### B. Experimental Results

Figure 5 describes the transitions from one axial symmetric contact. Figure 5-(a) shows an axial symmetric contact, where a regular triangle is in contact with the ground. Let us expand the icosahedron around the contacting triangle over the ground, as shown in Figure 5-(b). The blue regular triangle in the center represents the axial symmetric contact. We have observed a sequence of transitions caused by the application of air pressure to McKibben actuators. Through experiment, we find that a sequence of transitions can be categorized into two groups as:

AP axial $\rightarrow$ planar

AA axial $\rightarrow$ planar $\rightarrow$ axial

The former represents a single transition from the starting axial symmetric contact (blue triangle) to its neighboring planar symmetric contact (one of yellow triangles). The

(a)

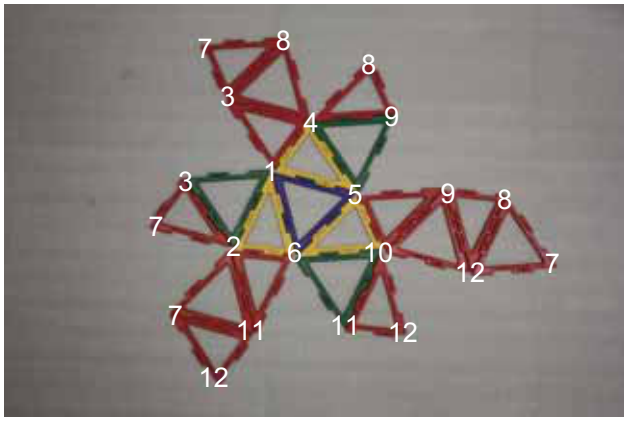


(b)

Fig. 5. Transitions from axial symmetric contact. (a) Starting axial symmetric contact. (b) The blue regular triangle in the center represents an axial symmetric contact. Three yellow isosceles triangles represent planar symmetric contacts, adjacent to the axial symmetric contact. Three green regular triangles represent axial symmetric contacts, each of which is adjacent to one of the planar symmetric contacts.

(a)

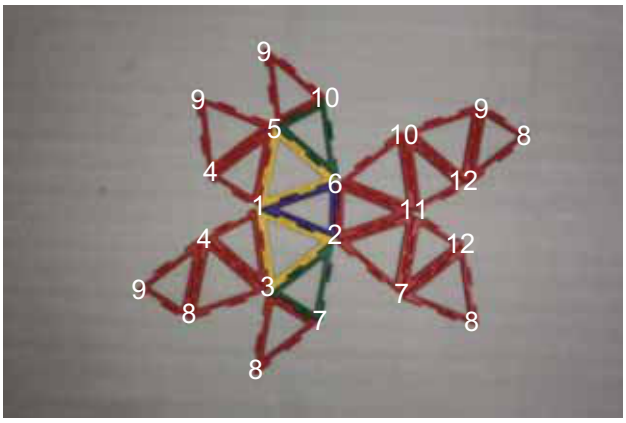


(b)

Fig. 6. Transitions from planar symmetric contact. (a) Starting planar symmetric contact. (b) The blue isosceles triangle in the center represents a planar symmetric contact. Three yellow regular triangles represent axial symmetric contacts, adjacent to the planar symmetric contact. Three green isosceles triangles represent planar symmetric contacts, each of which is adjacent to one of the axial symmetric contacts.

latter represents a sequence of two transitions, transition from the starting axial symmetric contact (blue triangle) to its neighboring planar symmetric contact (one of yellow triangles), followed by transition from the planar symmetric contact to its neighboring axial symmetric contact (green triangle). Here, the intermediate contact (yellow triangle) is unstable, resulting that the tensegrity robot passes through this contact and reaches to another stable state. Assume that a regular triangle $(1,5,6)$ is in contact with the ground. Category AP includes the following three transitions:

$$(1,5,6) \rightarrow (1,6,2),$$
$$(1,5,6) \rightarrow (5,1,4),$$
$$(1,5,6) \rightarrow (6,5,10).$$

Category AA includes the following three series of transitions:

$$(1,5,6) \rightarrow (1,6,2) \rightarrow (1,2,3),$$
$$(1,5,6) \rightarrow (5,1,4) \rightarrow (4,9,5),$$
$$(1,5,6) \rightarrow (6,5,10) \rightarrow (6,10,11).$$

Note that transitions from a regular triangle $(1,5,6)$ to its neighboring non-regular, isosceles triangles $(1,6,2)$, $(5,1,4)$, and $(6,5,10)$ are all possible.

Recalling that we are driving two McKibben actuators out of the 24 involved in a six-strut tensegrity robot, we have ${}_{24}C_2 = 276$ pairs of drivings of McKibben actuators. Starting from one axial symmetric contact, we have experimentally examined how many pair of the 276 can drive the robot. Table IV summarizes the experimental result. We find that 6 pairs can perform a transition involved in category AP. All transition can be realized by applying air pressure of 0.40 MPa. We find that 3 pairs can perform a sequence of transitions involved in category AA. All transition can be realized by applying air pressure of 0.50 MPa. The other 267 pairs cannot perform the rolling of the prototype. Namely, the tensegrity structure deforms but is not sufficient to perform any transition from the axial symmetric contact.

Figure 6 describes the transitions from one planar symmetric contact. Figure 6-(a) shows a planar symmetric contact, where a non-regular, isosceles triangle is in contact with the ground. Let us expand the icosahedron around the contacting triangle over the ground, as shown in Figure 6-(b). The blue isosceles triangle in the center represents the planar symmetric contact. We have observed a sequence of transitions caused by the application of air pressure to McKibben actuators. Through experiment, we find that a sequence of transitions can be categorized into two groups as:

TABLE IV

THE NUMBER OF ACTUATOR PAIRS THAT CAN PERFORM TRANSITIONS FROM AXIAL SYMMETRIC CONTACT

| pressure [MPa] | category AP | category AA |
|---|---|---|
| 0.50 | 0 | 0 |
| 0.10 | 0 | 0 |
| 0.15 | 0 | 0 |
| 0.20 | 0 | 0 |
| 0.25 | 0 | 0 |
| 0.30 | 0 | 0 |
| 0.35 | 0 | 0 |
| 0.40 | 6 | 0 |
| 0.45 | 0 | 0 |
| 0.50 | 0 | 3 |
| total | 6 | 3 |

TABLE V

THE NUMBER OF ACTUATOR PAIRS THAT CAN PERFORM TRANSITIONS FROM PLANAR SYMMETRIC CONTACT

| pressure [MPa] | category PA | category PP |
|---|---|---|
| 0.50 | 0 | 0 |
| 0.10 | 4 | 0 |
| 0.15 | 18 | 2 |
| 0.20 | 6 | 0 |
| 0.25 | 6 | 0 |
| 0.30 | 2 | 0 |
| 0.35 | 4 | 0 |
| 0.40 | 4 | 0 |
| 0.45 | 0 | 0 |
| 0.50 | 10 | 0 |
| total | 54 | 2 |

PA planar $\rightarrow$ axial

PP planar $\rightarrow$ axial $\rightarrow$ planar

The former represents a single transition from the starting planar symmetric contact (blue triangle) to its neighboring axial symmetric contact (one of yellow triangles). The latter represents a sequence of two transitions, transition from the starting planar symmetric contact (blue triangle) to its neighboring axial symmetric contact (one of yellow triangles), followed by transition from the axial symmetric contact to its neighboring planar symmetric contact (green triangle). Here, the intermediate contact (yellow triangle) is unstable, resulting that the tensegrity robot passes through this contact and reaches to another stable state. Assume that a non-regular, isosceles triangle $(1,6,2)$ is in contact with the ground. Category PA includes the following two transitions:

$$(1,6,2) \rightarrow (1,2,3),$$
$$(1,6,2) \rightarrow (1,5,6).$$

Category PP includes the following two series of transitions:

$$(1,6,2) \rightarrow (1,2,3) \rightarrow (2,7,3),$$
$$(1,6,2) \rightarrow (1,5,6) \rightarrow (6,5,10).$$

Note that transitions from a non-regular, isosceles triangle $(1,6,2)$ to its neighboring regular triangles $(1,2,3)$ and $(1,5,6)$ are possible, but transition to its neighboring non-regular, isosceles triangle $(11,2,6)$ is not possible. Experiment showed that any transition between two neighboring non-regular, isosceles triangles is not possible in this prototype.

Starting from one planar symmetric contact, we have experimentally examined how many pair of the 276 can drive the robot. Table V summarizes the experimental result. We find that 54 pairs can perform a transition involved in category PA. Four can be performed by applying air pressure of 0.10 MPa. We find that 2 pairs can perform a sequence of transitions involved in category PP. All transition can be realized by applying air pressure of 0.15 MPa. The other 220 pairs cannot perform the rolling of the prototype. Namely, the tensegrity structure deforms but is not sufficient to perform any transition from the planar symmetric contact.

### C. Discussion

We find that air pressure required to perform transitions involved in categories PA and PP is smaller than that in categories AP and AA. Note that after performing a transition in category PA, we have to perform transitions in categories AP or AA for successive rolling. This implies that we need larger air pressure for transitions in categories AP or AA, even though transitions in category PA require smaller air pressure. Contrary, our tensegrity robot can perform successive rolling by applying transitions in category PP repeatedly. Transitions in category PP can be performed by applying air pressure of 0.15 MPa. Namely, air pressure of 0.15 MPa can realize a sequence of transitions in PP category. Thus, rolling of a six-strut tensegrity robot should be based on transitions in PP category. In other words, the robot basically takes planar symmetric contacts alone in its stable state. If an axial symmetric contact happens due to uncertainties in the robot or the environment, we can apply any transition in category AP so that the contact between the robot and the ground returns back to any planar symmetric contact, then we can apply any transition in category PP again. Recall that transitions in category PP require air pressure of 0.15 MPa while transitions in category AP require 0.40 MPa. Thus, we find that our prototype can perform successive rolling by applying air pressure of 0.15 MPa basically. Only when an axial symmetric contact happens, we need to apply air pressure of 0.40 MPa.

Figure 7 shows snapshots of successive rolling of our prototype. Based on the above strategy, we can realize the successive rolling of our prototype of a six-strut tensegrity robot.

## V. CONCLUSIONS AND FUTURE WORKS

In this paper, we have experimentally investigated the rolling of a six-strut tensegrity robot driven by twenty-four pneumatic McKibben actuators. Based on the geometric description of a six-strut tensegrity robot, we have found that an axial symmetric contact between a tensegrity robot and a flat ground is represented by its corresponding regular triangle contacting to the ground while a planar symmetric contact is represented by its corresponding isosceles triangle contacting to the ground. We have experimentally investigated how

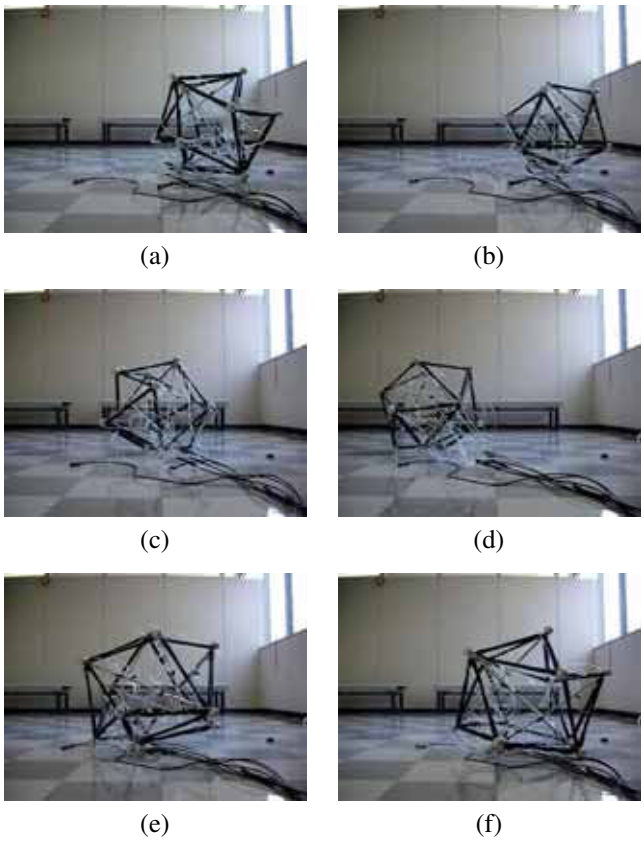

Fig. 7. Successive rolling of a six-strut tensegrity robot. The prototype can perform a successive rolling over a flat ground by applying air pressure to a sequence of actuator pairs.

much air pressure is required to perform transitions among contacts to conclude that transitions in category PP are suitable for successive rolling of a tensegrity robot.

Future works include

(a) planning of a sequence of driving actuators for a tensegrity robot to follow a given path,
(b) locomotion of a tensegrity robot over rough terrain,
(c) detection of orientation of a tensegrity robot,
(d) dynamic simulation of the rolling of a six-strut tensegrity robot,
(e) miniaturized pneumatic devices for internally powered locomotion of a tensegrity robot.

In this paper, we have found possible transitions among contacts and how much air pressure is needed for each transition. Based on this result, we will establish a method to determine a sequence of driving actuators that enables a tensegrity robot to follow a given path on the ground. We have focused on the tensegrity robot locomotion over a flat ground. We will apply the robot to the locomotion over rough terrain to investigate the performance of the robot experimentally. It is needed to detect the orientation of a tensegrity robot and to identify its contacting triangle to determine pneumatic McKibben actuators to be driven. We will apply a set of accelerometers to detect the orientation of a tensegrity robot. Also, we will build simulation of the rolling of a tensegrity robot so that we can assess the performance of the robot via simulation. Current prototype is externally powered; a compressor outside a tensegrity robot provides air pressure to drive pneumatic actuators. Our prototype has space enough to install the pneumatic system inside its body. In addition, we have already developed miniaturized pneumatic valves [20], which can be installed inside our tensegrity robot. We will apply this technology to our prototype so that the pneumatic system including air sources, control valves, and micro controllers are installed inside the robot.

## ACKNOWLEDGMENTS

This research was supported in part by JSPS Grant-in-Aid for Scientific Research 21760210.

## REFERENCES

[1] Otake, M., Inaba, M., and Inoue, H., *Development of a gel robot made of electro-active polymer PAMPS gel* Proc. IEEE Int. Conf. on Systems, Man, and Cybernetics, Vol. 2, pp.788–793, 1999.
[2] Y. Sugiyama and S. Hirai, *Crawling and Jumping by a Deformable Robot*, Int. J. of Robotics Research, Vol. 25, No.5–6, pp.603–620, 2004.
[3] H. Mochiyama, M. Watari, H. Fujimoto, *A robotic catapult based on the closed elastica and its application to robotic tasks*, Proc. IEEE/RSJ Int. Conf. on Intelligent Robots and Systems, pp.1508–1513, 2007.
[4] Steltz, E., Mozeika, A., Rodenberg, N., Brown, E., and Jaeger, H. M., *JSEL: Jamming Skin Enabled Locomotion*, Proc. IEEE/RSJ Int. Conf. on Intelligent Robots and Systems, pp.5672–5677, 2009.
[5] Petralia, M.T. and Wood, R.J., *Fabrication and analysis of dielectric-elastomer minimum-energy structures for highly-deformable soft robotic systems*, Proc. IEEE/RSJ Int. Conf. on Intelligent Robots and Systems (IROS), pp.2357–2363, 2010.
[6] DARPA Chemical Robots (ChemBots), http://www.darpa.mil/Our_Work/DSO/Programs/Chemical_Robots_%28ChemBots%29.aspx
[7] Mizuho Shibata, Fumio Saijyo, and Shinichi Hirai, *Crawling by Body Deformation of Tensegrity Structure Robots*, Proc. IEEE Int. Conf. on Robotics and Automation, pp.4375–4380, Kobe, May 12–17, 2009.
[8] Mizuho Shibata and Shinichi Hirai, *Moving strategy of tensegrity robots with semiregular polyhedral body*, Proc. 13th Int. Conf. Climbing and Walking Robots and the Support Technologies for Mobile Machines (CLAWAR 2010), Nagoya, Japan, Aug. 31–Sept. 3, 2010.
[9] *Website of K. Snelson*, http://www.kennethsnelson.net/.
[10] *Buckminster Fuller Institute*, http://www.bfi.org/.
[11] Wang Bin Bing, *Free-standing Tension Structures – From tensegrity systems to cable-strut systems*, Taylor & Francis, 0–415–33595–7, 2004
[12] J. Y. Zhang, M. Ohsaki, *Optimization Methods for Force and Shape Design of Tensegrity Structures*, Proc. 7th World Congresses of Structural and Multidisciplinary Optimization, pp.40–49, 2007.
[13] Robert E. Skelton and Mauricio C. de Oliveira, *Tensegrity Systems*, Springer, 978–0–387–74241–0, 2009.
[14] D. E. Ingber, *The Architecture of Life*, Scientific American, Jan., pp.30–39, 1998.
[15] J. B. Aldrich, R. E. Skelton, and K. Kreutz-Delgado, *Control Synthesis for a Class of Light and Agile Robotic Tensegrity Structures*, Proc. American Control Conference, pp.5245–5251, 2003.
[16] C. Paul, J. W. Roberts, H. Lipson, and F. J. V. Cuevas, *Gait Production in a Tensegrity Based Robot*, Proc. Int. Conf. on Advanced Robotics, pp.216–222, 2005.
[17] C. Paul, F. J. Valero-Cuevas, and H. Lipson, *Design and Control of Tensegrity Robots for Locomotion*, IEEE Trans. on Robotics, Vol. 22, No. 5, pp.944–957, 2006.
[18] M. Arsenault and C. M. Gosselin, *Kinematic and Static Analysis of a Three-degree-of-freedom Spatial Modular Tensegrity Mechanism*, Int. Journal of Robotics Research, Vol. 27, No. 8, pp.951–966, 2008.
[19] *Virtual Polyhedra*, http://www.georgehart.com/virtual–polyhedra/vp.html.
[20] Sumadi Jien, Shinichi Hirai, and Kenshin Honda, *Miniaturization Design of Piezoelectric Vibration-Driven Pneumatic Unconstrained Valves*, Journal of Robotics and Mechatronics, Vol. 22, No. 1, pp.91–99, February, 2010.